Anatomy of plastic events in magnetic amorphous solids

H. George E. Hentschel, Itamar Procaccia, and Bhaskar Sen Gupta
Department of Chemical Physics, The Weizmann Institute of Science, Rehovot 76100, Israel
(Received 25 January 2015; revised manuscript received 19 January 2016; published 16 March 2016)

Plastic events in amorphous solids can be much more than just "shear transformation zones" when the positional degrees of freedom are coupled nontrivially to other degrees of freedom. Here we consider magnetic amorphous solids where mechanical and magnetic degrees of freedom interact, leading to rather complex plastic events whose nature must be disentangled. In this paper we uncover the anatomy of the various contributions to some typical plastic events. These plastic events are seen as Barkhausen noise or other "serrated noises." Using theoretical considerations we explain the observed statistics of the various contributions to the considered plastic events. The richness of contributions and their different characteristics imply that in general the statistics of these serrated noises cannot be universal, but rather highly dependent on the state of the system and on its microscopic interactions.

DOI: 10.1103/PhysRevE.93.033004

I. INTRODUCTION

Modeling the mechanical properties of amorphous solids is an active subject of current research, requiring a detailed understanding of the many-body processes that occur in such system when subjected to external strains. External strains can be mechanical, magnetic, or electric, depending on the properties of the amorphous solid in question. The responses of amorphous solids to such external strains is usually not smooth, giving rise to "serrated" plots of stress vs strain, energy vs strain, magnetization vs external magnetic field, etc. A lot of effort was spent on characterizing the probability distribution functions of such serrated responses. In the context of magnetic jumps this is referred to as Barkhausen noise [1–6] but other serrated noises were studied as well [7]. In a number of cases strong claims of universality were made.

Recently we have analyzed in some detail model amorphous solids in which there is a significant coupling between mechanical and magnetic properties [8–11]. Doing so we realized that the characterization of the physics of plastic events can be quite demanding; there is more in these events than what meets the eye at first impression. The aim of this paper is to highlight the somewhat complex anatomy of plastic events in such systems, with a word of caution to researchers in the field that similar complexity may arise in other systems as well, and reasonable modeling should take this into account. In particular, we will conclude below that in general one should not expect universal probability distribution functions since the statistics of the serrated responses depend on many details of the microscopic interactions and on the state of the system.

Deferring all details to the next section, we motivate the present paper by showing in Fig. 1 a scatter plot of the values of energy drops ΔU during plastic events when the system is strained by an external magnetic field. The scatter plot is shown as a function of the magnetization jump Δm that occurs simultaneously with the energy drop. First, one sees that for a given Δm one has a wide distribution of ΔU values. Second, these values of the energy drops fall in different groups, with a strange intense line and two triangular groups that are only partly overlapping. Understanding such scatter plots and their implications on the physics of the solid is what we mean by "the anatomy of plastic events." A theory of plasticity in such system should include also the understanding of the statistical distribution of such events. The density of points in every little box of size $d\Delta U d\Delta m$ in Fig. 1 is proportional to the joint probability $P(\Delta U,\Delta m)d\Delta U d\Delta m$. Understanding how this probability distribution function is determined by the different physical process requires a theory of the anatomy of plastic events. The aim of this paper is to provide such a theory for one particular model of amorphous magnetic glass. Other models will require a similar approach.

In Sec. II we present the model that was introduced recently and analyzed for some of its aspects in Refs. [8–11]. Section III deals with the notion of plastic events, both under external mechanical strain and under external magnetic field. The anatomy of the plastic events that occur under magnetic straining is studied in Sec. IV, in which we provide the numerical analysis, a theory, and a comparison between the two. In Sec. V we discuss briefly the anatomy of plastic events under mechanical straining, including the implications to magnetostriction. The last section offers a summary and a discussion.

II. A MODEL OF A MAGNETIC AMORPHOUS SOLID WITH STRONG LOCAL ANISOTROPY

The model Hamiltonian was introduced in [8] and analyzed further in [9–12]. The magnetic part of the model is in the spirit of the Harris, Plischke and Zuckerman (HPZ) Hamiltonian [13] but with a number of important modifications. These modification were made to bring the model closer to the physics of amorphous magnetic solids [8]. The first major difference is that the particles in the present case are not pinned to a lattice. We write the Hamiltonian as

$$U(\{\boldsymbol{r}_i\},\{\boldsymbol{S}_i\}) = U_{\rm mech}(\{\boldsymbol{r}_i\}) + U_{\rm mag}(\{\boldsymbol{r}_i\},\{\boldsymbol{S}_i\}), \qquad (1)$$

where $\{\boldsymbol{r}_i\}_{i=1}^N$ are the two-dimensional positions of N particles in an area L^2 and $\boldsymbol{S}_i$ are spin variables. The mechanical part $U_{\rm mech}$ is chosen to represent a glassy material with a binary mixture of 65% particles A and 35% particles B, with Lennard-Jones potentials having a minimum at positions $\sigma_{AA} = 1.175\,57$, $\sigma_{AB} = 1.0$, and $\sigma_{BB} = 0.618\,034$ for the corresponding interacting particles [14]. These values are chosen to guarantee good glass formation and avoidance of crystallization. The energy parameters chosen are $\epsilon_{AA} = \epsilon_{BB} = 0.5$, $\epsilon_{AB} = 1.0$, in units for which the Boltzmann

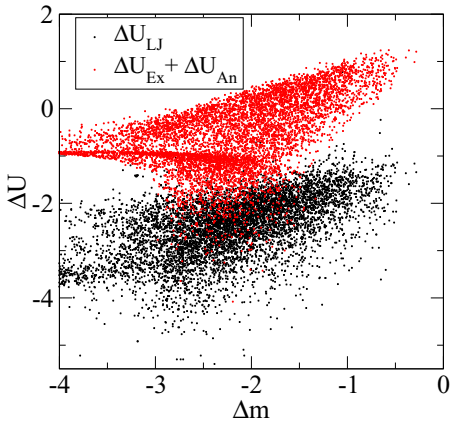

FIG. 1. Log-log scatter plot of the value of the energy drops ΔU as a function of the simultaneous changes Δm in the magnetization. These occur when the magnetic field is ramped up and down to form the hysteresis loop of the Barkhausen noise. Note that here and below the scatter plots are in double logarithmic scale.

constant equals unity. All the potentials are truncated at distance 2.5σ with two continuous derivatives. N_A particles A carry spins $\boldsymbol{S}_i$; the N_B B particles are not magnetic. Of course $N_A + N_B = N$. We choose the spins $\boldsymbol{S}_i$ to be classical xy spins; the orientation of each spin is then given by an angle ϕ_i with respect to the direction of the external magnetic field which is along the x axis.

The magnetic part of the potential energy takes the form [8]

$$U_{\rm mag}(\{\boldsymbol{r}_i\},\{\boldsymbol{S}_i\}) = -\sum_{\langle ij\rangle} J(r_{ij})\cos(\phi_i-\phi_j) - \sum_i K_i \cos^2[\phi_i-\theta_i(\{\boldsymbol{r}_i\})] - \mu_A B\sum_i \cos(\phi_i). \quad (2)$$

Here $r_{ij} \equiv |\boldsymbol{r}_i - \boldsymbol{r}_j|$ and the sums are only over the A particles that carry spins. Notice that in the present model the exchange parameter $J(\boldsymbol{r}_{ij})$ is a function of a changing interparticle position (either due to affine motions induced by an external strain or an external magnetic field or due to nonaffine particle displacements, and see below). Thus randomness in the exchange interaction is coming from the random positions $\{\boldsymbol{r}_i\}$, whereas the function $J(\boldsymbol{r}_{ij})$ is not random. We choose the monotonically decreasing form $J(x) = J_0 f(x)$ where $f(x) \equiv \exp(-x^2/0.28) + H_0 + H_2x^2 + H_4x^4$ with $H_0 = -5.51\times 10^{-8}$, $H_2 = 1.68\times 10^{-8}$, $H_4 = -1.29\times 10^{-9}$. This choice cuts off $J(x)$ at $x = 2.5$ with two smooth derivatives. Note that we need to have at least two smooth derivatives in order to compute the Hessian matrix below. Finally, in our case $J_0 = 3$.

Another major difference with the HPZ model is that in the present case the local axis of anisotropy θ_i is *not* selected randomly, but is determined by the local structure. Recall that in a crystalline solid the easy axis is determined by the symmetries of the lattice. In an amorphous solid the arrangement of particles changes from one position to the other, and we need to find the local easy axis by taking this local structure into account. Define the matrix $\boldsymbol{T}_i$:

$$T_i^{\alpha\beta} \equiv \sum_j J(r_{ij}) r_{ij}^\alpha r_{ij}^\beta \Big/ \sum_j J(r_{ij}). \quad (3)$$

Note that we sum over all the particles that are within the range of $J(r_{ij})$; this is sufficient to take into account the arrangement of the local neighborhood of the ith particle. The matrix $\boldsymbol{T}_i$ has two eigenvalues in two dimensions that we denote as $\kappa_{i,1}$ and $\kappa_{i,2}$, $\kappa_{i,1} \geqslant \kappa_{i,2}$. The eigenvector that belongs to the larger eigenvalue $\kappa_{i,1}$ is denoted by $\hat{\boldsymbol{n}}$. The easy axis of anisotropy is given by $\theta_i \equiv \sin^{-1}(|\hat{n}_y|)$. Finally the coefficient K_i which now changes from particle to particle is defined as

$$K_i \equiv \tilde{C}\Big[\sum_j J(r_{ij})\Big]^2 (\kappa_{i,1}-\kappa_{i,2})^2\,, \quad \tilde{C} = K_0/J_0\sigma_{AB}^4. \quad (4)$$

The parameter K_0 determines the strength of this random local anisotropy term compared to other terms in the Hamiltonian. For most of the data shown below we chose $K_0 = 5.0$. The form given by Eq. (4) ensures that for an isotropic distribution of particles $K_i = 0$. Due to the glassy random nature of our material the direction θ_i is random. In fact we will assume below (as can be easily tested in the numerical simulations) that the angles θ_i are distributed randomly in the interval $[-\pi,\pi]$. It is important to note that ramping the magnetic field does *not* change this flat distribution and we will assert that the probability distribution $P(\theta_i)$ can be simply taken as

$$P(\theta_i)d\theta_i = \frac{d\theta_i}{2\pi}. \quad (5)$$

In order to prepare our system we start with the random initial positions of 2000 particles in a square box of volume V with periodic boundary condition and temperature $T = 1.2$ at density $\rho = 0.976$. We use Monte Carlo simulation to equilibrate the system at this temperature. The system was then cooled down to $T = 0.6$ and equilibrated. Next the temperature was reduced down to $T = 0.2$ in steps of $\Delta T = 0.1$ followed by equilibration after each step. Finally the athermal limit is reached by cooling it down to $T = 0.001$ with steps of $\Delta T = 0.001$ where thermal effects can be completely neglected. At this point we begin to ramp the external magnetic field in the x direction in small steps of $\Delta B = 10^{-4}$ followed by energy minimization using conjugate gradient method. This quasistatic increase in magnetic field eliminates any effects of rate of ramping. It was checked that the jump in magnetization Δm and energy ΔU remains unchanged when ΔB is reduced to 10^{-5} and 10^{-6}. We have checked in the numerical simulations that Eq. (5) is valid to a high approximation at all values of B. The last term in Eq. (2) is the interaction with the external field B. We have chosen $\mu_A B$ in the range $[-0.08,0.08]$. At the two extreme values all the spins are aligned along the direction of $\boldsymbol{B}$.

In passing we should comment on the chosen parameters in the model. Our guiding line was to choose parameters such that the magnetostriction coefficient is of the order of what is known in laboratory materials. Decreasing K_0 results in much smaller magnetostriction coefficients and vice versa. We did not aim at modeling a particular material, and our interest here, as before, is in the generic properties of amorphous solids with strong local anisotropy.

III. WHAT IS PLASTICITY?

It is well known that plasticity in crystalline solids is carried by defects, such as dislocations, whose glide under external strains is dissipative, leading to energy loss. What are the mechanisms of energy loss in amorphous solids is less well known, although research in the last two decades has shed considerable light on the fundamental physics of plasticity in amorphous solids [15–20]. In the present system we can have two distinct external agents that can strain the system, i.e., mechanical strain and magnetic field. Such external strain can be studied in systems having finite or zero temperature. Since we are interested in the anatomy of plastic events we opt for the latter; temperature fluctuations tend to mask the clear-cut plastic events that are recognized at $T = 0$. To keep the system at $T = 0$ we must also ramp the external strain or the magnetic field quasistatically to allow the system to remain in mechanical equilibrium at all times, without heating effects. In such conditions it is completely clear what are the instabilities that are responsible to plastic events.

The response of our system to external strain, be it mechanical or magnetic, is reversible and smooth as long as the system is mechanically and magnetically stable. This is the case as long as the Hessian matrix $\mathcal{H}$ has only positive eigenvalues. In the present case $\mathcal{H}$ takes on the form [8]

$$\mathcal{H} = \begin{pmatrix} \frac{\partial^2 U}{\partial \boldsymbol{r}_i \partial \boldsymbol{r}_j} & \frac{\partial^2 U}{\partial \boldsymbol{r}_i \partial \phi_j} \\ \frac{\partial^2 U}{\partial \phi_i \partial \boldsymbol{r}_i} & \frac{\partial^2 U}{\partial \phi_i \partial \phi_j} \end{pmatrix}. \tag{6}$$

The system loses stability when at least one of the eigenvalues of $\mathcal{H}$ goes to zero. When this happens, there appears an instability that results in a discontinuous change in stress, in energy, and in magnetization. These discontinuities appear simultaneously in all three quantities at the same values of B. These are irreversible plastic events that take the system from one minimum in the energy landscape through a saddle-node bifurcation to another minimum in the energy landscape where again all the eigenvalues of $\mathcal{H}$ are positive. In Ref. [8] we derived an exact equation for the dependence of any eigenvalue λ_k on B for a fixed external strain, which reads

$$\left.\frac{\partial \lambda_k}{\partial B}\right|_\gamma = c_{kk}^{(b)} - \sum_\ell \frac{a_\ell^{(b)}\left[b_{kk\ell}^{(r)} + b_{kk\ell}^{(\phi)}\right]}{\lambda_\ell}. \tag{7}$$

The precise definition of all the coefficients is given explicitly in Ref. [8]. Generically, when one eigenvalue, say λ_P, approaches zero, all the other terms in Eq. (7) remain bounded, leading to the approximate equation

$$\left.\frac{\partial \lambda_P}{\partial B}\right|_\gamma \approx \frac{\text{const}}{\lambda_P}. \tag{8}$$

In such generic situations the eigenvalue is expected to vanish following a square-root singularity, $\lambda_P \sim (B_p - B)^{1/2}$ where B_p is the value of the external magnetic field where the eigenvalue vanishes. The reader should be aware of the fact that at some special values of B it may happen that the coefficient const in Eq. (8) vanishes at the instability leading to an exponent different from $1/2$ [9]. This nongeneric feature hardly changes the considerations of the present paper.

It is interesting to examine what happens to the eigenfunctions $\boldsymbol{\Psi}^k$ which are associated with the eigenvalues λ_k as the instability is approached. The answer is that all the eigenfunctions of $\mathcal{H}$ are delocalized far from the instability, but the one eigenfunction $\boldsymbol{\Psi}^P$ associated with $\lambda_P \to 0$ gets localized on $n \ll N$ particles. A typical projection of $\boldsymbol{\Psi}^P$ close to the instability on the particle positions and on the spins is shown in the two panels of Fig. 2. We see that the nonaffine movement of the particles is very similar to the standard "Eshelby-like" quadrupolar event that is so typical to amorphous solids. The projection on the spin degrees of freedom shows that a patch of spins had changed its orientation (magnetic flip of a domain). Note that in the present model this patch is compact. This is the nature of the event that is associated with the Barkhausen noise in our case. The reader should be aware, however, of the fact that the

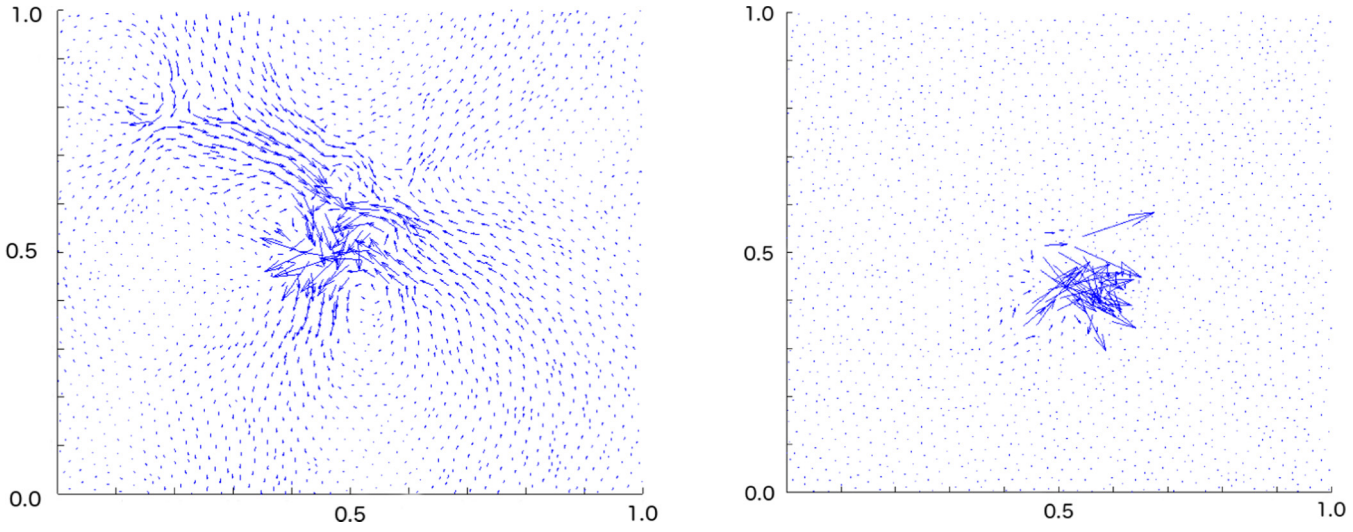

FIG. 2. The projection of the eigenfunction $\boldsymbol{\Psi}^P$ associated with the eigenvalue λ_P which vanishes at the instability, projected on the particle positions and on the spins in the left and right panels, respectively. The left panel shows a typical nonaffine displacement field associated with a plastic event, having the quadrupolar structure of an Eshelby solution. The right panel shows that the same event is associated with a colocal flip of spins, leading to the change δM of the Barkhausen noise.

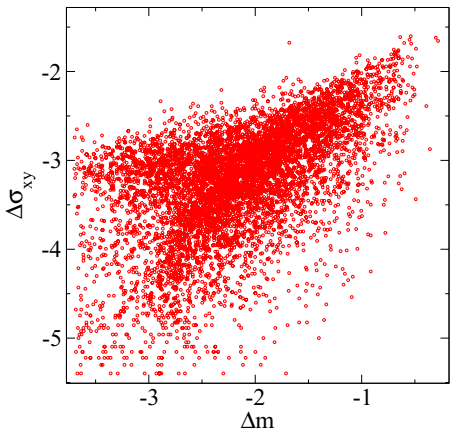

FIG. 3. Scatter plot of the value of the stress drops $\Delta\sigma$ as a function of the simultaneous changes Δm in the magnetization. These occur when the magnetic field is ramped up and down to form the hysteresis loop of the Barkhausen noise.

addition of long range dipole-dipole interactions can change this qualitatively [21], leading to elongated magnetic domains and a different mechanism of Barkhausen noise due to the movement of domain boundaries [6].

IV. THE ANATOMY OF PLASTICITY

The interesting physics of plasticity in this model stems from the fact that the Hessian matrix (6) couples the positional to the magnetic degrees of freedom. Thus a plastic drop in stress and energy will be usually coupled also to a change in the magnetization. Whether one strains the system with a mechanical strain or a magnetic field, the plastic drops will be composite processes in which all the degrees of freedom contribute to the nonaffine response. In this section we focus on those events that are triggered by the magnetic field as the straining agent. To expose the anatomy of the plastic events we present the data as a scatter plot of the drops in energy or in stress as a function of the magnetization change Δm. The first was shown in Fig. 1 and the second is shown here as Fig. 3. As before, we see that also the values of the stress drops organize into two distinct groups that are, however, not nonoverlapping.

A. Detailed analysis of the energy drops

Our first task is to rationalize the distributions that appear in figures such as Figs. 1 and 3. Focusing as an example on the energy drops, we return to the Hamiltonian and find out which of the terms is responsible to which group of energy drop values in these figures. This separation is demonstrated in Fig. 4, where the energy drop is assigned to four different contributions to the Hamiltonian, i.e., the Lennard-Jones positional degrees of freedom, the exchange interaction, the anisotropy energy, and finally the interaction with the magnetic field. Obviously the combination of the scatter plots in Fig. 4 will lead to what was shown as Fig. 1. The same decomposition can be done for the stress drops but for the sake of brevity we focus here on understanding the results shown in Fig. 4; a similar analysis for the stress drops is implied.

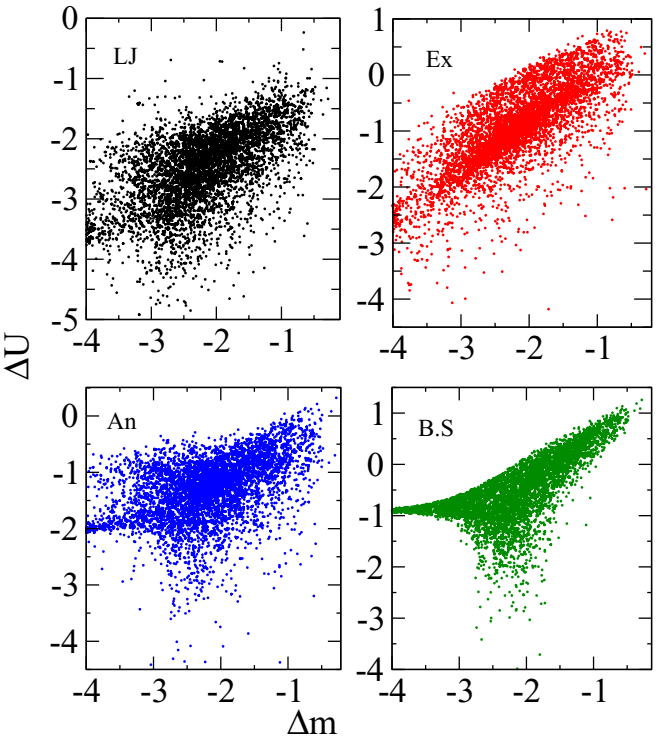

FIG. 4. The four distinct contributions namely the mechanical (LJ), exchange (Ex), anisotropic (An) and magnetic field (B.S) to energy drops in plastic events. The combination of all these scatter plots should yield the data in Fig. 1.

To understand what we see we will invoke the result of the previous work [11] in which the distribution $P(\Delta m)$ was measured over three orders of magnitude $10^{-3.5} < \Delta m < 10^{-0.5}$. These magnetization changes involved flips of magnetic domains of between $10^0 < \Delta n < 10^3$ particles. This probability distribution function (PDF) was found to be well fitted in this regime by a form

$$P(\Delta m) = \frac{\exp(-A\Delta m)}{\Delta m} f(\Delta m), \tag{9}$$

where the exponential decay rate A is analytically computed and the function $f(\Delta m)$ is evaluated explicitly:

$$f(\Delta m) = \frac{2}{\pi}\int_0^{\sqrt{2/\Delta m - 1}} dz \frac{\exp[-(\Delta m/2\langle x\rangle)z^2]}{z^2+1}. \tag{10}$$

The reader is referred to Ref. [11] for the details of the derivation of this form.

To make the connection to our present data we need to discuss the conditional distribution $P(\Delta U|\Delta m)$ in terms of which the joint distribution

$$P(\Delta U, \Delta m) = P(\Delta U|\Delta m)P(\Delta m) \tag{11}$$

can be written.

We shall start with the general form for the energy drop

$$\Delta U = \sum_{i=1}^{n} u_i, \tag{12}$$

where u_i is the energy change (both mechanical and magnetic) associated with the slip of the ith spin in the flipping domain

and n is the number of flipping spins. We assume that each spin flip contributes to Δm where

$$\Delta m = \mu_A \sum_i \Delta \cos(\phi_i), \tag{13}$$

and thus

$$n \sim C\Delta m, \tag{14}$$

with some unknown constant C. Thus ΔU is a sum of n random variables, and using the central limit theorem we can assume a Gaussian form for the conditional probability

$$P(\Delta U|\Delta m) = \frac{1}{\sqrt{2\pi\sigma^2}} \exp -(\Delta U - \langle \Delta U \rangle)^2/(2\sigma^2), \tag{15}$$

where both the average energy drop $\langle \Delta U \rangle = \langle \Delta U \rangle(\Delta m)$ and the variance of the energy drops $\sigma^2 = \sigma(\Delta m)^2$ are functions of Δm.

We can now introduce two exponents ζ_1 and ζ_2 by

$$\begin{aligned} \langle \Delta U \rangle(\Delta m) &= K_1 \Delta m^{\zeta_1}, \\ \sigma^2(\Delta m) &= K_2 \Delta m^{\zeta_2}. \end{aligned} \tag{16}$$

One of the purposes of these notes is to estimate these exponents ζ_1 and ζ_2.

Now the total energy drop can be separated into its individual mechanical and magnetic contributions

$$\begin{aligned} \Delta U &= \Delta U^{\text{mech}} + \Delta U^{\text{mag}} \\ &= \Delta U^{\text{mech}} + \Delta U^{\text{ex}} + \Delta U^{\text{anis}} + \Delta U^{b}, \end{aligned} \tag{17}$$

where ΔU^{mech} is the mechanical contribution to the energy drop, while the spin contribution can be separated into exchange ΔU^{ex}, anisotropic ΔU^{anis}, and magnetic field ΔU^{b} contributions, and depending on the spin Hamiltonian for the metallic glass [which in our case is Eq. (2)] may lead to different exponents.

Let us therefore analyze the consequences of Eq. (12) carefully. First we note that

$$\langle \Delta U \rangle(\Delta m) = \sum_{i=1}^{n} \langle u_i \rangle, \tag{18}$$

and thus if a nonzero $\langle u_i \rangle = \langle u \rangle$ exists we would find that $\langle \Delta U \rangle(\Delta m) \sim \Delta m$ or $\zeta_1 = 1$. On the other hand, if there exists a contribution consisting of n random variables with zero mean, then we might expect that contribution to scale like $\sim \Delta m^{1/2}$ or $\zeta_1 = 1/2$. The important point to note is that by measuring ζ_1 the physics underlying the spin flips can be found.

To estimate the variance of the fluctuations $\sigma^2 = \langle \Delta U^2 \rangle - \langle \Delta U \rangle^2$ we write, using Eq. (12),

$$\sigma(\Delta m)^2 = \sum_{i=1}^{n} \sum_{j=1}^{n} [\langle u_i u_j \rangle - \langle u_i \rangle \langle u_j \rangle]. \tag{19}$$

Thus while $\langle \Delta U \rangle$ only depends on the additive contribution of n random variables, the variance also depends on the correlation of different spins within the flipped domain. To see the consequence of these correlations, let us consider first the case where the spins i and j are uncorrelated. In that case $\sigma(\Delta m)^2 = n[\langle u^2 \rangle - \langle u \rangle^2] \sim \Delta m$ or $\zeta_2 = 1$. On the other hand, in the limit of strong correlations between spins in the flipped domain $[\langle u_i u_j \rangle - \langle u_i \rangle \langle u_j \rangle] \neq 0$ and as a consequence $\sigma(\Delta m)^2 \sim \Delta m^2$ or $\zeta_2 = 2$. It is also possible that the clean scaling described above may not exist but rather several mechanisms are mixed. Only simulations and data analysis can answer these questions.

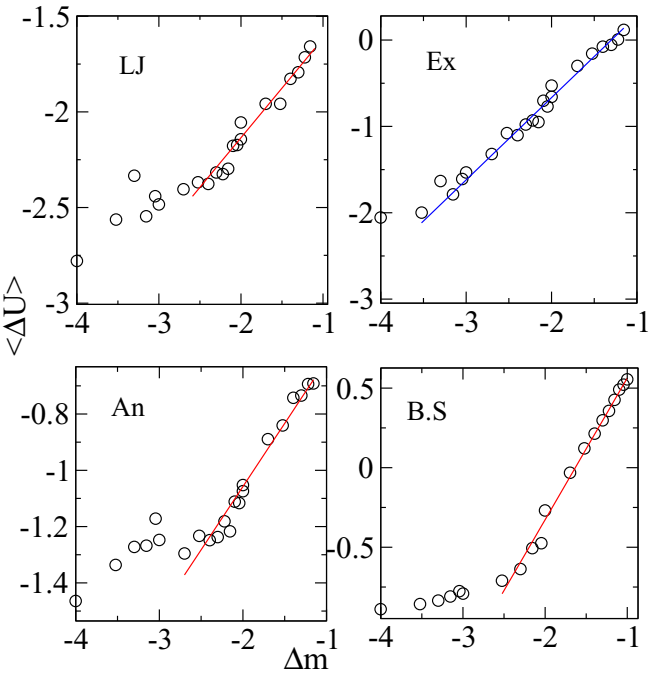

FIG. 5. The mean of $\langle \Delta U \rangle$ as a function of Δm for the four different contributions that play a role in our system.

Analyzing the data shown in Fig. 4 we could approximate each of the four conditional PDFs in the form

$$P_i(\Delta U|\Delta m) \approx e^{-[\Delta U - K_1(\Delta m)^{\zeta_1}]^2/K_2(\Delta m)^{\zeta_2}}. \tag{20}$$

The best fits for the exponents ζ_1 and ζ_2 and for the constant σ are provided in Table I.

The quality of the fits is demonstrated in Figs. 5 and 6. The exponents agree with our expectations of being 1/2 or 1, except for the variance of the Lennard-Jones contribution in Fig. 6. We note, however, that the amplitude of the Lennard-Jones ΔU is two orders of magnitude less than the other contributions and therefore we are close to the noise level and cannot trust this particular measurement. The smallness of this contribution arises from the fact that the straining here is done magnetically and the positions of the particles do not change that much.

One should note that the different contributions to the energy drops are *not* independent, and therefore the Gaussian

TABLE I. The best fit values of ζ_1 and ζ_2 for different energy terms. Note that the exponent of 0.77 is not explained theoretically but the data for this particular contribution is small, close to the noise level. All the exponents are given with error bars ± 0.004.

	LJ	Ex	An	B.S
ζ_1	0.52	0.96	0.47	0.98
ζ_2	0.77	1.09	0.97	1.12

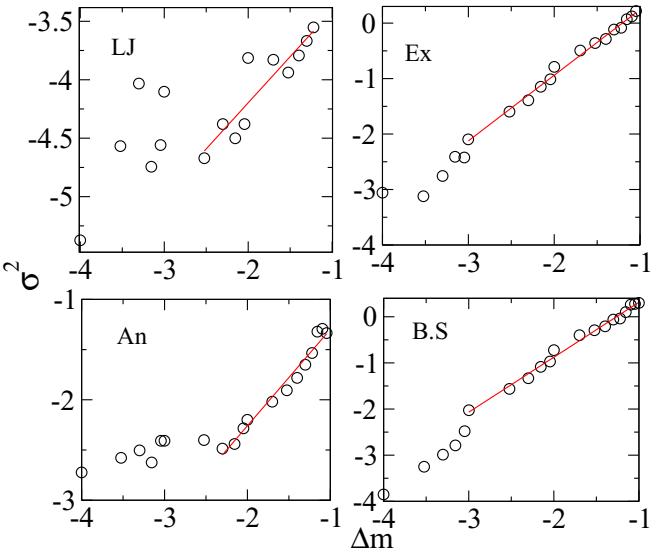

FIG. 6. The variance in the energy changes as a function of Δm for the four different contributions that play a role in our system.

approximation can be only approximate. In Fig. 7 we show a typical fit of a Gaussian PDF to the exchange contribution, demonstrating that the Gaussian approximation is acceptable.

At this point we want to use the results of Ref. [11] in which an analytic form for the probability to see a magnetic jump of Δm was proposed. To this aim we will attempt to find an analytic approximation to the PDF $P(\Delta U|\Delta m)$. We start by stating the obvious, i.e., that

$$\langle \Delta U|\Delta m\rangle = \sum_{i=1}^{4} \langle \Delta U_i(\Delta m)\rangle, \tag{21}$$

where the sum runs over the four contributions identified above. Next, the variance Σ^2 of the conditional probability

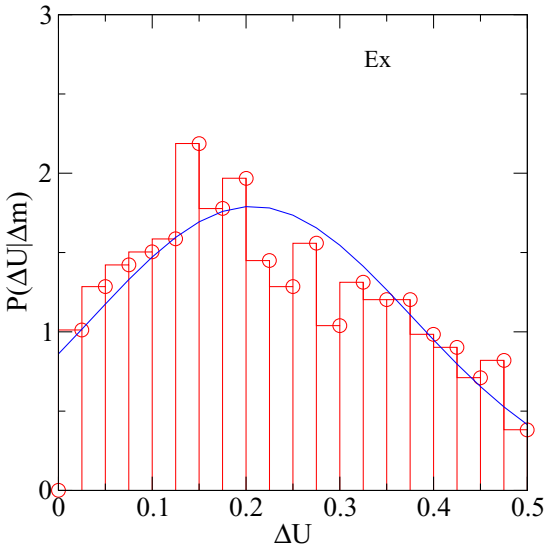

FIG. 7. A typical example of the Gaussian fit to the data of the exchange contribution to the energy drops. Similarly acceptable Gaussian fits are available for all the other contributions.

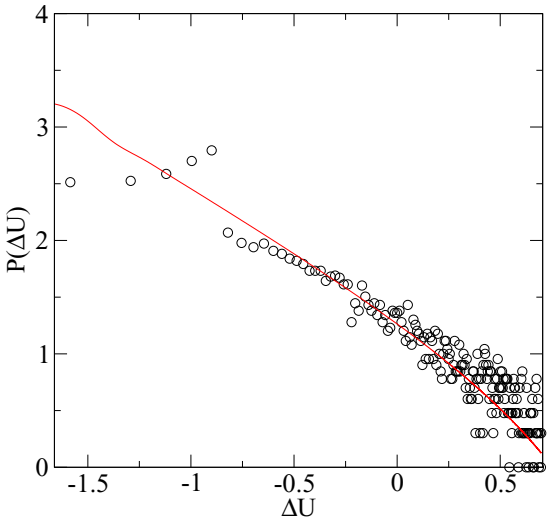

FIG. 8. Comparison of the direct calculation of $P(\Delta U)$ in plastic events due to straining with the magnetic field to the reconstruction of the same quantity from the anatomical dissection of this quantity and the independent knowledge of $P(\Delta m)$ [11].

can be obtained as

$$\Sigma^2 \equiv \left\langle \left(\sum_{i=1}^{4} \Delta U_i(\Delta m) - \langle \Delta U|\Delta m\rangle \right)^2 \right\rangle. \tag{22}$$

Having the variance we can construct the Gaussian approximation

$$P(\Delta U|\Delta m) \approx \frac{1}{\Sigma\sqrt{2\pi}} e^{-\{[\sum_{i=1}^{4} \Delta U_i(\Delta m) - \langle \Delta U|\Delta m\rangle]^2/2\Sigma^2\}}. \tag{23}$$

Finally we write $P(\Delta U)$ in the form

$$P(\Delta U) = \int d\Delta m\, P(\Delta U|\Delta m) P(\Delta m). \tag{24}$$

Now we use the analytic form of $P(\Delta m)$ from Ref. [11] and compute the integral (24) numerically. The comparison of this reconstruction of the PDF of ΔU to its direct numerical calculation is shown in Fig. 8.

The conclusion of this exercise is that providing the anatomical details of the plastic events can help in understanding the statistics of energy or stress drops. We do not repeat in this paper the exercise for the stress drops since it follows verbatim the same steps.

V. STRAINING MECHANICALLY

A similar richness in the anatomy of plastic events is found when the system is strained mechanically [10]. Even though we strain mechanically the coupling between positional and spin degrees of freedom results again in having a change in magnetization together with drops in energy and in stress. In Figs. 9 and 10 we show a typical plot of energy, stress, and magnetization vs external strain, for zero magnetic field and for a finite magnetic field. Note that in the first case the total magnetization remains zero on the average, with the flips in magnetization Δm being negative or positive with equal probability. For finite magnetic field magnetization is

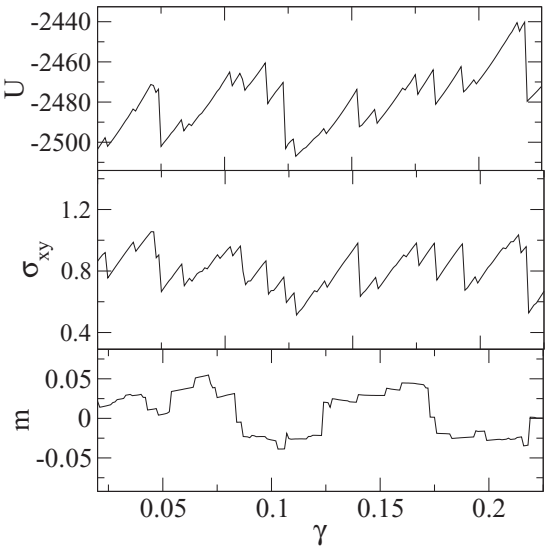

FIG. 9. Typical dependence of the energy, stress, and magnetization for zero external magnetic field. Note that all the plastic events occur simultaneously for all quantities. In the present case the magnetization is fluctuating up and down around a zero mean value.

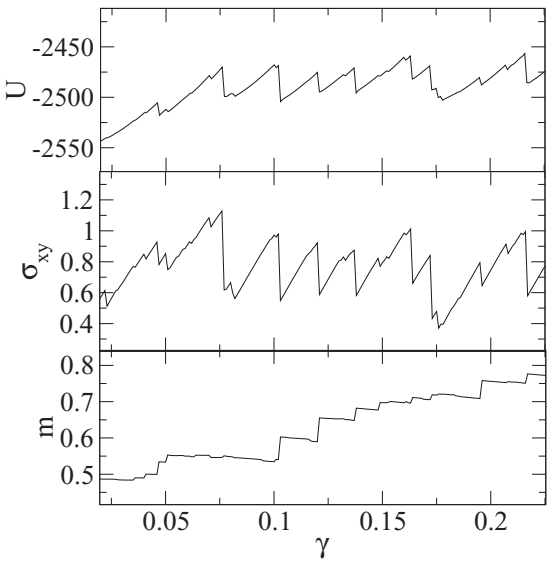

FIG. 10. Typical dependence of the energy, stress, and magnetization for external magnetic field $B = 0.01$. In the present case the plastic events cause the magnetization to increase; we called this phenomenon "plasticity induced magnetization" [10].

accumulated in the direction of the magnetic field at each plastic event. As before with ramping the magnetic field we see that also with mechanical strain the plastic events couple mechanical and magnetic degrees of freedom. The drops in energy are occurring as a result of plastic instabilities at the same values of γ as the drops in stress and magnetization. The mechanism is the same, i.e., an eigenvalue of the Hessian matrix hits zero punctuating the smooth curves of energy, stress, or magnetization with sharp drops of irreversible events.

To understand the serrated response curve of the energy or the stress one needs again to search for the anatomy of the events, displaying carefully the contribution of each physical mechanism for either energy or stress drop. Since we did not compute independently the "Barkhausen noise" $P(\Delta m)$ in this case we do not repeat the exercise for the case of mechanical straining. We stress, however, that any interested researcher must pay attention to the rich physics that is underlying the serrated "noisy" character of the data shown in Figs. 9 and 10.

VI. SUMMARY AND CONCLUSIONS

The main conclusion of this paper is that *characterizing* and *understanding* the statistics of serrated noise is not necessarily the same. Even if we can plot the PDFs of energy drops or of magnetic jumps and measure the exponent that is associated with their log-log plot, it does not mean that we uncovered the intricate physics that underlies the phenomenon. We have seen here that even the simplest coupling between mechanical and magnetic degrees of freedom results in a multitude of contributions to the energy changes upon plastic events. Each contribution comes with its own statistics, its own exponent, and its own amplitude. Of course, once we have the full information of all the contributions we can reconstruct the PDF of any wanted quantity (cf. Fig. 8). The full information is, however, not always available in experimental systems. Thus great care is called for interpreting the observed statistics of serrated noises. In particular, we should stress that changing conditions (such as zero or nonzero magnetic field in Figs. 9 and 10) may change the statistics of the serrated noise. The amplitude of the various contributions to the observed serrated response can depend on the state of the system, etc. Thus universal statistics is expected to be the exception rather than the rule. Rather, a careful analysis of the physics underlying the observed response is called for.

ACKNOWLEDGMENT

This work has been supported in part by an ERC "ideas" grant STANPAS.

[1] H. Barkhausen, Phys. Z. **20**, 401 (1919).
[2] D. Spasojevic, S. Bukvić, S. Milosević, and H. E. Stanley, Phys. Rev. E **54**, 2531 (1996).
[3] P. Le Doussal, A. A. Middleton, and K. J. Wiese, Phys. Rev. E **79**, 050101(R) (2009).
[4] O. Perković, K. Dahmen, and J. P. Sethna, Phys. Rev. Lett. **75**, 4528 (1995).
[5] J. P. Sethna, K. A. Dahmen, and C. R. Myers, Nature (London) **410**, 242 (2001).
[6] G. Durin and S. Zapperi, in *The Science of Hysteresis*, edited by G. Bertotti and I. Mayergoyz (Elsevier, Amsterdam, 2006), Vol. II, pp. 181–267.
[7] E. K. H. Salje, X. Wang, X. Ding, and J. Sun, Phys. Rev. B **90**, 064103 (2014).

[8] H. G. E. Hentschel, V. Ilyin, and I. Procaccia, Europhys. Lett. **99**, 26003 (2012).
[9] R. Dasgupta, H. G. E. Hentschel, I. Procaccia, and B. S. Gupta, Europhys. Lett. **104**, 47003 (2013).
[10] H. G. E. Hentschel, I. Procaccia, and B. Sen Gupta, Europhys. Lett. **105**, 37006 (2014).
[11] H. G. E. Hentschel, V. Iliyn, I. Procaccia, and B. Sen Gupta, J. Stat. Mech. (2014) P08020.
[12] R. Gutierrez, B. S. Gupta, and I. Procaccia, Phys. Rev. B. **90**, 094112 (2014).
[13] R. Harris, M. Plischke, and M. J. Zuckerman, Phys. Rev. Lett. **31**, 160 (1973).
[14] R. Brüning, D. A. St-Onge, S. Patterson, and W. Kob, J. Phys.: Condens. Matter **21**, 035117 (2009).
[15] L. Malandro and D. J. Lacks, J. Chem. Phys. **110**, 4593 (1999).
[16] A. Tanguy, J. P. Wittmer, F. Leonforte, and J-L. Barrat, Phys. Rev. B **66**, 174205 (2002).
[17] C. E. Maloney and A. Lemaitre, Phys. Rev. Lett. **93**, 016001 (2004); **93**, 195501 (2004).
[18] S. Karmakar, E. Lerner, and I. Procaccia, Phys. Rev. E **82**, 026105 (2010).
[19] H. G. E. Hentschel, S. Karmakar, E. Lerner, and I. Procaccia, Phys. Rev. E **83**, 061101 (2011).
[20] E. Lerner and I. Procaccia, Phys. Rev. E **79**, 066109 (2009).
[21] A. K. Dubey, H. G. E. Hentschel, P. K. Jaiswal, C. Mondal, I. Procaccia, and B. Sen Gupta, Europhys. Lett. **112**, 17011 (2015).